Case 13585

Eurorad••

Granulosa cell tumor of the ovary:
functional MRI

Published on 26.04.2016

Authors: Athina C. Tsili, Christina Naka, Vasilios
Maliakas, Maria I. Argyropoulou

Patient: 38 years, female

Clinical History:

A 38-year-old woman was referred for MRI of the pelvis due to infertility.

Imaging Findings:

MRI examination revealed the presence of a mainly solid right ovarian mass
(Fig. 1-3), measuring 2.9 x 2.1 x 3.3 cm. The lesion was well-defined, mainly isointense on both T1 and T2-weighted images (Fig. 1), when compared to the normal myometrium. Dynamic contrast-enhanced images showed strong and heterogeneous mass enhancement, with an earlier and steeper rise than that of the normal myometrium and a curve type 3 (Fig. 2). Hyperintense areas on T2-weighted images, with absence of contrast enhancement, proved to represent internal cysts on pathology. Restricted diffusion was seen within the mass, which was detected mainly hyperintense and hypointense on DWI and ADC maps, respectively (Fig. 3). Neither peritoneal seeding nor pelvic lymphadenopathy was detected.

Discussion:

Background
Histology following right salpingo-oophorectomy reported an early-stage (FIGO IA) granulosa cell tumour (GCT) of the ovary.
Ovarian GCT accounts for less than 5% of ovarian malignancies [1]. It represents the commonest malignant sex cord–stromal tumour and the most common oestrogen-producing ovarian neoplasm. Most patients have an excellent prognosis [1].
Imaging Perspective
GCTs of the ovary have variable histopathologic characteristics resulting in a spectrum of imaging findings [2-4]. They may have the appearance of solid masses, tumors with haemorrhagic or fibrotic changes, multilocular cystic lesions filled with watery fluid or haemorrhage, or completely cystic tumours [2-4]. Functional MRI techniques, including dynamic contrast-enhanced (DCE) MRI and diffusion-weighted imaging (DWI) have been reported to improve the diagnostic assessment of ovarian masses [5]. There is paucity in the English literature regarding the functional MRI characteristics of ovarian GCTs.
DCE-MRI might provide useful information in differentiating among benign, borderline, and invasive epithelial tumours [6-11]. Invasive ovarian tumours usually show early and strong enhancement, with an initial rise steeper than that of myometrium, defined as "curve type 3" [6-11]. A correlation between the early enhancement patterns of

ovarian epithelial tumours and tumoral angiogenic status including pericyte coverage index and vascular endothelial growth factor receptor expression has been reported [8]. Quantitative DCE-MRI has been reported as useful in the differentiation between malignant and benign ovarian tumours, with malignancies displaying higher tissue blood flow, higher blood volume fraction, higher area under the enhancing curve and lower interstitial volume fraction compared to benign tumours [9].

ADC mapping is reported less useful in the characterization of ovarian masses because of the considerable overlap of mean and lowest ADC values [5, 11-16]. This mainly reflects the increased mean ADC detected in ovarian malignancies and the decreased lowest ADC in benign lesions. The presence of desmoplastic stroma and/or fluid between papillary projections may be the cause of increased mean ADC in malignant tumours. Bundles and storiform patterns of spindle cells in fibromas, thick proteinaceous or bloody products in endometriomas, keratinoid substance in mature cystic teratomas may cause decreased lowest ADC in benign ovarian lesions [11-16]. However, DWI signal intensity in combination with morphologic findings has been reported as an accurate tool for differentiating complex adnexal masses. Specifically, the presence of a solid component with intermediate T2 signal and high b 1, 000 signal intensity was associated with a positive likelihood-ratio of 4.5 for a malignant ovarian tumour [12].

Differential Diagnosis List: Granulosa cell tumour of the ovary, Serous cystadenocarcinoma, Endometrioid carcinoma, Malignant germ cell tumour

Final Diagnosis: Granulosa cell tumour of the ovary

References:

Outwater EK, Wagner BJ, Mannion C, McLarney JK, Kim B (1998) Sex cord-stromal steroid cell tumors of the ovary. Radiographics 18:1523-1546 (PMID: 9821198)

Morikawa K, Hatabu H, Togashi K, Kataoka ML, Mori T, Konishi J (1997) Granulosa Cell Tumor of the Ovary: MR Findings. J Comput Assist Tomogr 21:1001-1004 (PMID: 9386298)

Jung SE, Rha SE, Lee JM, Park SY, Oh SN, Cho KS, Lee EJ, Byun JY, Hahn ST (2005) CT and MRI Findings of Sex Cord-Stromal Tumor of the Ovary. AJR Am J Roentgenol 185:207-215 (PMID: 15972425)

Kim SH, Kim SH (2002) Granulosa Cell Tumor of the Ovary: Common Findings and Unusual Appearances on CT and MR. J Comput Assist Tomogr 26:756-61 (PMID: 12439311)

Wakefield JC, Downey K, Kyriazi S, deSouza NM (2013) New MR Techniques in Gynecologic Cancer. AJR Am J Roentgenol 200:249–260 (PMID: 23345344)

Van Vierzen PB, Massuger LF, Ruys SH, Barentz JO (1998) Borderline ovarian malignancy: ultrasound and fast dynamic MR findings. Eur J Radiol 28:136-142 (PMID: 9788017)

Thomassin-Naggara I, Darai E, Cuenod CA, Rouzier R, Callard P, Bazot M (2008) Dynamic Contrast-Enhanced Magnetic Resonance Imaging: A Useful Tool for Characterizing Ovarian Epithelial Tumors. J Magn Reson Imaging 28:111-120 (PMID: 18581400)

Thomassin-Naggara I, Bazot M, Darai E, Callard P, Thomassin J, Cuenod CA (2008) Epithelial ovarian tumors: value of dynamic contrast-enhanced MR imaging and correlation with tumor angiogenesis. Radiology 248:148-159 (PMID: 18458244)

Thomassin-Naggara I, Balvay D, Aubert E, Daraï E, Rouzier R, Cuenod CA, Bazot M (2012) Quantitative dynamic contrast-enhanced MR imaging analysis of complex adnexal masses: a preliminary study. Eur Radiol 22:738–745 (PMID: 22105841)

Bernardin L, Dilks P, Liyanage S, Miquel ME, Sahdev A, Rockall A (2912) Effectiveness of semi-quantitative multiphase dynamic contrast-enhanced MRI as a predictor of malignancy in complex adnexal masses: radiological and pathological correlation. Eur Radiol 22:880–890 (PMID: 22095438)

Thomassin-Naggara I, Toussaint I, Perrot N et al (2011) Characterization of complex adnexal masses: value of adding perfusion- and diffusion-weighted MR imaging to conventional MR imaging. Radiology 258:793–803 (PMID: 21193596)

Thomassin-Naggara I, Darai E, Cuenod CA et al (2009) Contribution of diffusion-weighted MR imaging for predicting benignity of complex adnexal masses. Eur Radiol 19:1544–1552 (PMID: 19214523)

Fujii S, Kakite S, Nishihara K, et al (2008) Diagnostic Accuracy of Diffusion-Weighted Imaging in Differentiating Benign From Malignant Ovarian Lesion. J Magn Reson Imaging 28:1149-1156 (PMID: 18972356)

Bakir B, Bakan S, Tunaci M et al (2010) Diffusion-weighted imaging of solid or predominantly solid gynaecological adnexial masses: is it useful in the differential diagnosis?. Br J Radiol 84:600–611 (PMID: 21081581)

Katayama M, Masui T, Kobayashi S, Ito T, Sakahara H, Nozaki A, et al (2002) Diffusion-weighted echo planar imaging of ovarian tumors: is it useful to measure apparent diffusion coefficients?. Comput Assist Tomogr 26:250-256 (PMID: 11884782)

Kaji Y, Matsuo M, Matsuki M, Yoshida M, Hayashi M, Nanno H, Koshiyama M, Fujii H, Maruyama K, Takizawa O, Sugimura K (2002) Cystic Ovarian Lesions in SSFP Imaging. Magn Reson Med Sci 15:183-189 (PMID: 16082143)

Figure 1

a
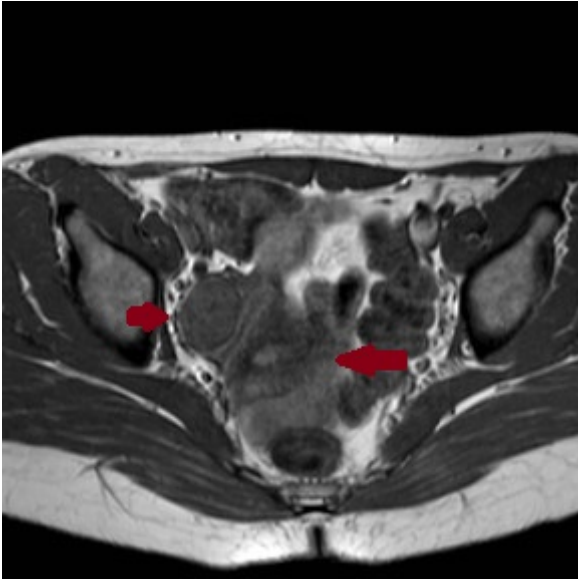
Description: Transverse T1-weighted image shows an ovoid, well-delineated right adnexal mass lesion (arrow), mainly isointense to the normal uterus (long arrow). **Origin:** Tsili A, Department of Radiology, University of Ioannina, Greece.
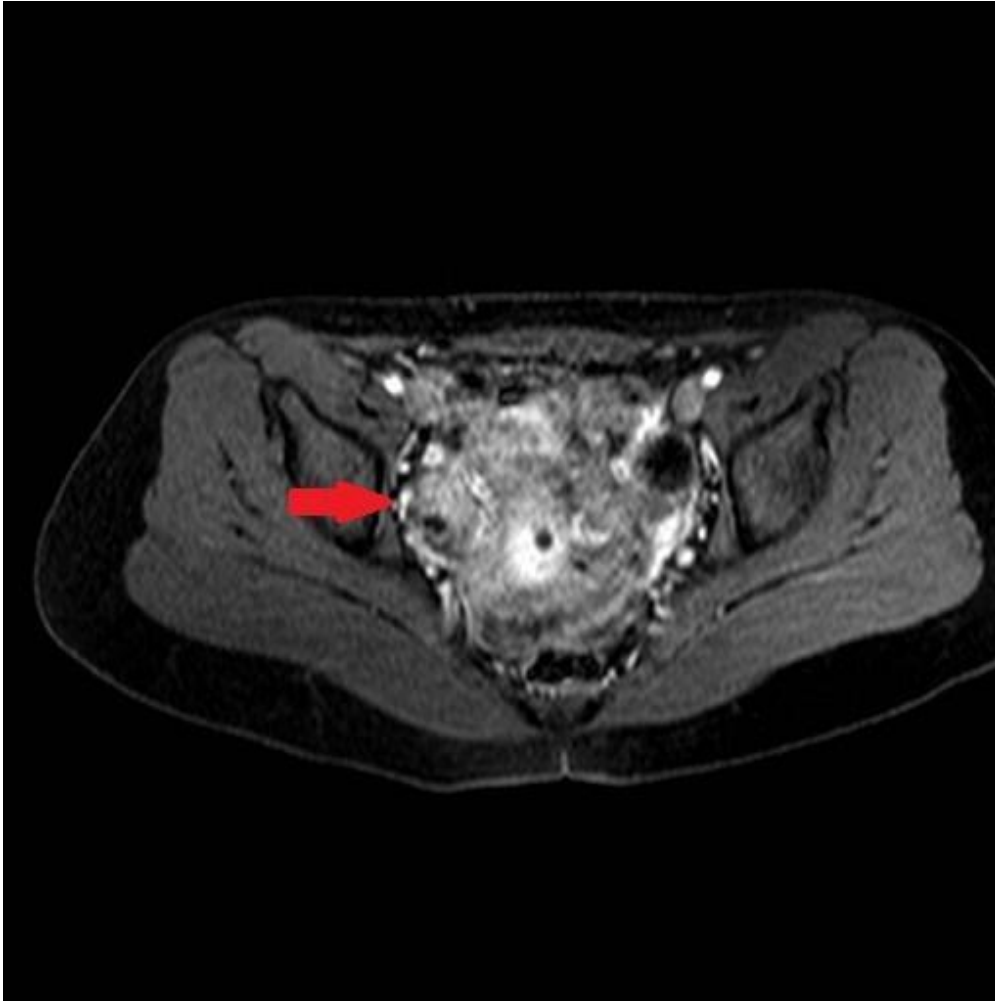
b

Description: Transverse T2-weighted image depicts inhomogeneous right adnexal mass (arrow), mainly isointense to normal myometrium (not shown on these images). Small hyperintense area (long arrow) within the lesion, corresponding to internal cyst on pathology. **Origin:** Tsili A, Department of Radiology, University of Ioannina, Greece.
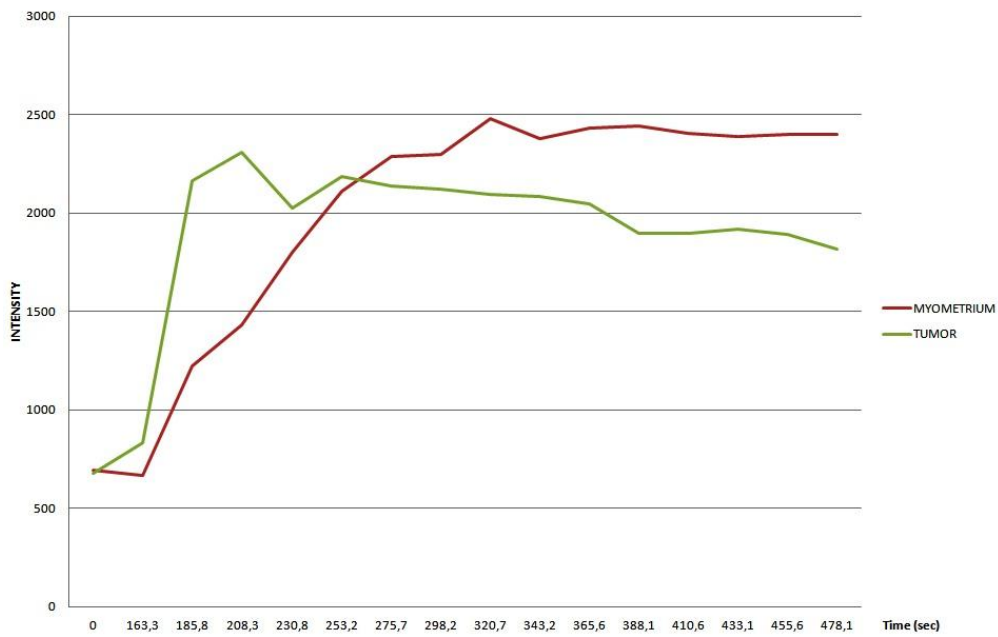
Figure 2

a

Description: Dynamic contrast-enhanced fat-suppressed T1-weighted image (early phase) reveals strong and heterogeneous lesion enhancement (arrow). **Origin:** Tsili A, Department of Radiology, University of Ioannina, Greece.
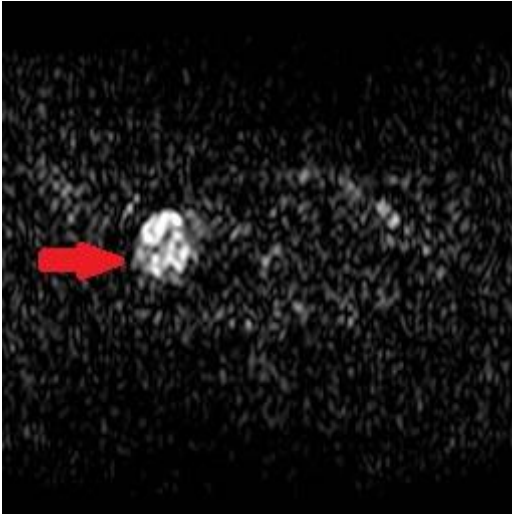
b

Description: Time signal intensity curves of tumour and normal myometrium. **Origin:** Tsili A, Department of Radiology, University of Ioannina, Greece.
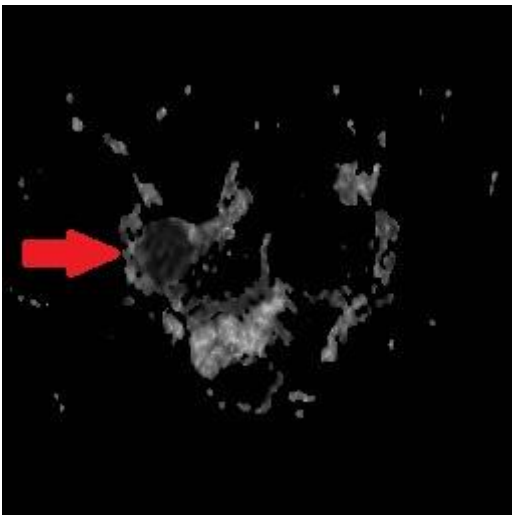
Figure 3

a

Description: Transverse DWI image (b= 800 s/mm2) shows lesion hyperintensity (arrow). **Origin:** Tsili A, Department of Radiology, University of Ioannina, Greece.

b

Description: Corresponding ADC map demonstrates the tumour (arrow) as hypointense. The mean ADC value within the mass is 0.76 ×10–3 mm2/s. **Origin:** Tsili A, Department of Radiology, University of Ioannina, Greece.